J. Fluid Mech. (1978), *vol.* 89, *part* 4, *pp.* 665–671
Printed in Great Britain

Laser speckle measurements of transient Bénard convection

By P. G. SIMPKINS AND T. D. DUDDERAR
Bell Laboratories, Murray Hill, New Jersey 07974

(Received 24 January 1978)

Quantitative velocity measurements of unsteady convection in a Bénard cell suddenly cooled from above to a supercritical Rayleigh number are reported. The results are obtained by a novel application of laser speckle photography adapted for the study of fluid dynamics. This technique allows two-dimensional full-field velocity information to be obtained solely from a selected plane within the volume of moving liquid at any given instant in time. The convective rolls are found to be regular and oriented parallel to the short side of the cell. The number of rolls within the cell is approximately twice as great as the number reported for steady conditions. The maximum vertical velocity distribution is observed to be a sinusoidal function of the horizontal distance with a detectable third-harmonic component.

1. Introduction

Recent communications by Grousson & Mallick (1977), Barker & Fourney (1977) and the present authors (1977) have described the successful development of an optical technique for making velocity measurements in a fluid-dynamic environment using laser speckle fields. Coincidentally each of these studies reproduced the classical results of Poiseuille. However, because the Poiseuille flow field is unidirectional and steady it does not adequately demonstrate the versatility of the technique. Therefore reported herein are some observations of a more complicated flow field: the convective rolls in a Bénard cell suddenly cooled from above to a supercritical Rayleigh number. The intention here is not to report a thorough study of the Bénard problem. Rather, the purpose is to illustrate the scope and sensitivity of this novel development of the technique known as laser speckle photography (LSP) in the course of making a contribution to the transient Bénard problem.

Velocity measurements of Bénard flow fields have also been made recently by Dubois & Bergé (1978) using laser–Doppler anemometry, another technique employing scattered laser light. That technique provides a time history of a single velocity component at one point in space. In contrast, the present laser speckle technique provides a full-field two-dimensional velocity distribution at one instant in time.

2. Experimental technique

The speckle phenomenon, i.e. the grainy appearance of a diffusely reflecting surface illuminated by a laser beam, arises because of the high degree of coherence of laser light; see Dainty (1975). This grainy appearance is caused by constructive and destructive interference of coherent light scattered from a surface element whose roughness is

large compared with the wavelength. When photographed the speckle size can be estimated from the Rayleigh resolution criterion

$$s \approx 1{\cdot}2\lambda f(1+m), \tag{1}$$

where λ is the wavelength, f the lens f-number and m the magnification. In the application of LSP to quasi-static problems a double-exposed photograph of the speckle pattern, or specklegram, is taken before and after a disturbance has been introduced. Since the typical size of the speckle in the image plane is $O(10\ \mu\text{m})$, high resolution film is used to record the specklegrams. When the specklegram is interrogated, i.e. illuminated by a narrow beam of coherent light, a regular pattern of fringes, analogous to Young's fringes, appears within the resulting diffraction halo provided that the speckle patterns correlate. The angular separation α of the fringes is given by

$$\sin\alpha = \lambda/dm, \tag{2}$$

where d is the displacement normal to the fringe orientation. The technique permits measurement of displacements greater than s; the upper limit beyond which correlation between the individual speckles ceases is about $20s$. Fringe patterns appear upon interrogation only if the two individual speckle patterns correlate. Changes which alter the speckle distribution other than by displacing it reduce the correlation and suppress or eliminate the fringe pattern.

In the present study the phenomenon is not quasi-static but dynamic, and the subject is transparent. Consequently, no diffusely reflecting surface exists from which to record the specklegrams. This difficulty is overcome by lightly seeding the fluid with white latex paint ($\sim$ 0·01 ml per l) and shaping the illuminating coherent light into a thin sheet 25×1 mm as it passes through the medium. Thus an effective surface is generated from which speckle patterns of the side-scattered light may in principle be recorded. Because the fluid is in motion it is necessary to make each of the double exposures in as short a time as possible to effectively arrest the movement. The integrated movement which occurs between these exposures is the effective disturbance being evaluated, provided that the duration between pulses is large compared with the exposure time. If this duration is known, and is sufficiently short, the magnitude and direction of the local in-plane velocity components can be found. Very short time exposures of high intensity light pulses are needed to overcome the low efficiency of the side-scattering technique. Consequently a 6 J double-pulsed Q-switched ruby laser capable of pulse separations as short as 1 μs is used as a light source.

LSP measurements of the convective flow in a Bénard cell containing an aqueous solution of 50 % glycerine by volume have been performed with the experimental arrangement shown in figure 1. The cell, with interior dimensions of $127 \times 90 \times 25$ mm, is constructed from 6 mm thick optical glass plates on an aluminium base 50 mm thick. The illuminated plane is parallel to the longest side of the cell and at a distance z into the interior. The temperature at the centre of the base plate is monitored by a chromel–alumel thermocouple connected to a digital recorder. The rigid top surface is an aluminium boat filled with crushed ice. Thus the boundary conditions on the solution in the cell are insulating walls and conducting horizontal boundaries. In all the tests, the fluid in the cell is allowed to stabilize initially at room temperature ($23 \pm 0{\cdot}2$ °C) before the boat is filled with crushed ice. The specklegrams are recorded

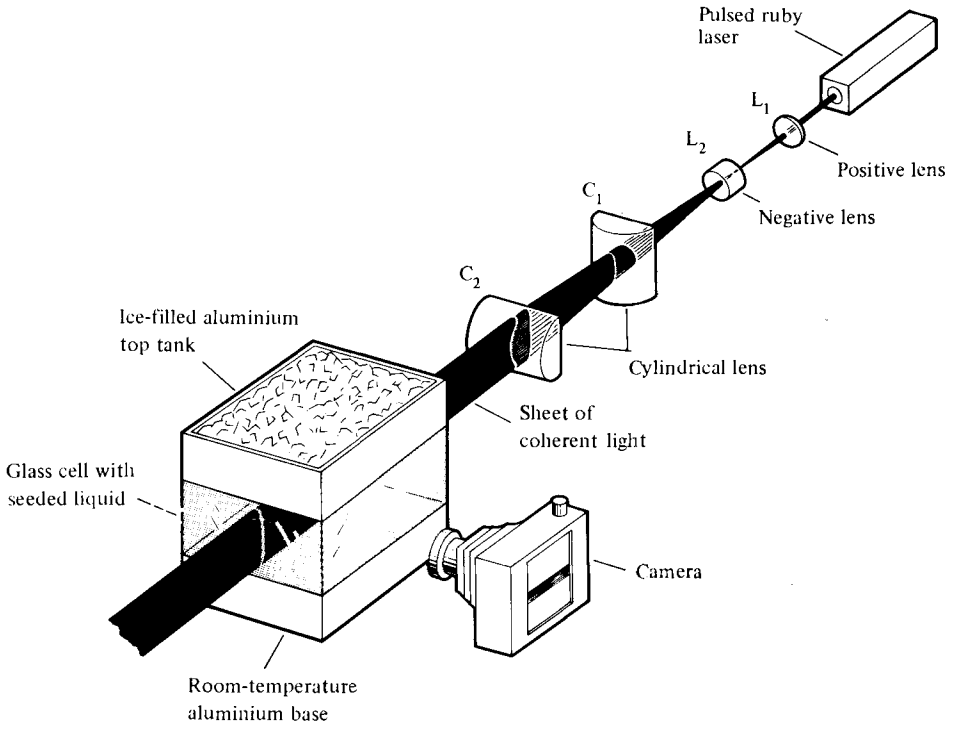

FIGURE 1. Experimental arrangement for side-scattering LSP in a Bénard cell.

2·5–3 min later, when the temperature of the aluminium base has fallen to 20 °C, so the effective temperature difference θ is 20 °C and $d\theta/dt = 1{\cdot}1 \pm 0{\cdot}1$ °C/min.

At 20 °C the aqueous solution has the following physical properties (see Perry & Chilton 1973, pp. 87, 213):

density, $\rho = 1{\cdot}1263$ g/cm^3,
viscosity, $\mu = 7 \times 10^{-2}$ g/cm s,
thermal diffusitivity, $\kappa \approx 1{\cdot}2 \times 10^{-3}$ cm^2/s,
coefficient of volume expansion, $\alpha \approx 3{\cdot}5 \times 10^{-4}$ °C^{-1}.

The last two properties are approximated by the mean of the values for pure glycerine and water. Thus, for $\theta = 20$ °C, the Rayleigh number $Ra = g\alpha\theta h^3/\kappa\nu$ is $O(10^6)$ and the Prandtl number ν/κ is approximately 50. Here ν is the kinematic viscosity μ/ρ and h is the depth. Therefore supercritical conditions occur initially in the cell and quasi-stable convective rolls are to be anticipated; see Koschmieder (1974). A number of visual observations with the cell fully illuminated by a CW laser beam were made during the course of these experiments. These consistently indicated the presence of a two-dimensional roll structure parallel to the shorter side walls. These findings contrast with those of Krishnamurti (1968), who reported visual observations of hexagonal cells for Bénard experiments with changing mean temperature. These differences are reconcilable when it is recognized that Krishnamurti's experiments were conducted close to Ra_c and for $d\theta/dt = 3$ °C/h, whereas the current data were obtained at supercritical values of $Ra = O(10^6)$ and for $d\theta/dt = 60$ °C/h. Palm (1975) has noted that, while stable hexagonal cells will form in the vicinity of Ra_c, only

two-dimensional rolls are stable for large supercritical values of Ra as occur here. As time progresses the Rayleigh number decreases and the conditions in the cell approach the critical state. This is due to the reducing temperature difference θ as heat is transported into the cold upper surface. The time scale on which this change occurs is large, however, compared with the duration of the experiments.

3. The measurements

A number of double-exposed specklegrams were recorded with 10 ms pulse separations. Several diffraction-fringe patterns obtained by interrogating a typical specklegram taken with $z = 16$ mm at different points in the field 20 mm below the top of the cell are shown in figure 2 (plate 1). Note that as the point of interrogation is moved across the field the separation of the fringes first increases and then decreases while their orientation rotates through 180°. These fringe patterns illustrate the variations in the magnitude and direction of the velocity vector along the line described by the path of the interrogating beam as it traverses the rolls. A thorough interrogation on a 1 mm by 2 mm grid has also been performed on this specklegram. The corresponding velocity distribution from these measurements is shown in figure 3 for the visible half of the cell. Four distinct rolls and evidence of a fifth near the end wall are apparent. The end-wall roll could not be determined because speckle correlation in that region is reduced by the off-axis limitations of the camera lens. However, the measurements nearest the wall and the lateral position of the first definitive roll together with visual observations strongly support the interpretation that another roll exists in the vacant space in figure 3. The sensitivity of the technique is also apparent as velocities as small as 0·4 mm/s are discernible from the specklegram. Velocities much greater than the value of 4 mm/s shown here can also be measured using the same pulse separation. Furthermore, changing the duration of the pulse separation changes the range of application to cover greater or lesser mean velocities as needed.

The results in figure 3 also indicate that during the time scales under investigation there is no detectable motion in a layer near the cold surface. This broad low velocity region in the vicinity of the cold surface is attributable to the large change in the viscosity of the solution which occurs near 0 °C. The strong dependence of viscosity on temperature results in a thicker boundary layer and lower velocities near the cold surface and a thinner boundary layer and higher velocities near the hot surface. Consequently the velocity distribution is skewed towards the hot surface, as is seen in the figure. Similar observations of this type of behaviour have been made by Elder (1965). The anomalous behaviour which occurs in pure water near 4 °C does not appear to persist in the 50 % aqueous glycerol solution. Nevertheless, the layer does affect the nature of the convective rolls beneath it for two reasons: first, the effective depth of the cell is reduced by approximately 30 %, and second, the top surface boundary condition has been relaxed since in effect it is no longer a solid interface. Consequently, the relevant Rayleigh number for the roll structure is $O(10^5)$ and the heat transfer to the top is reduced. These aspects of the study will be discussed in greater detail in a later communication.

A number of observations can be made regarding the Bénard convection in the suddenly cooled situation. The results agree with earlier observations, see Koschmieder (1966), and the prediction of Davis (1967) that the finite rolls in a rectangular

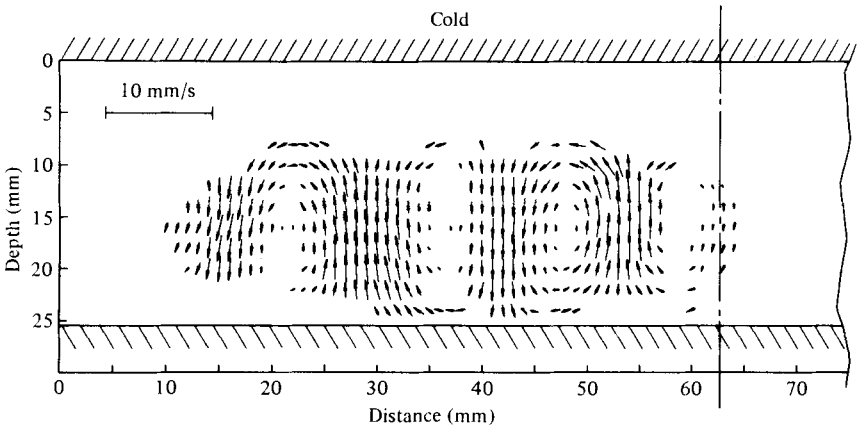

FIGURE 3. Full-field velocity distribution in half of the cell for an effective Rayleigh number $O(10^5)$.

geometry are parallel to the shorter side walls. However, since ten rolls occur in the cell the roll wavelength $\frac{1}{2}\Lambda$ is about half that observed in earlier steady-state measurements by Stork & Müller (1972). Here the normalized wavelength $\Lambda/h \approx 1{\cdot}0$ has been confirmed on five other specklegrams taken in repeated experiments at comparable times after the thermal gradient was established. Consequently, the rolls observed do not appear to be square in cross-section but rather are elongated vertically. Other studies of the transient problem also indicate that the roll wavelength is a function of the supercritical Rayleigh number and varies accordingly with time. Koschmieder (1969) observed that, when a supercritical temperature difference is suddenly applied to a liquid layer between conducting horizontal boundaries, motions with wavelengths shorter than $\Lambda/h = 2{\cdot}016$ are produced. Foster (1965) found a similar behaviour at high supercritical Rayleigh numbers when a fluid is suddenly cooled from above, as in the present case. Davis (1978, private communication) has suggested that the roll wavelength is determined by the scale of the thermal boundary layer at the onset of the instability. Since this scale is determined by the rate of change of the thermal gradient it is reasonable to conclude that the latter accounts for the decrease in wavelength consistently observed in transient situations.

Figure 4, derived from the results shown in figure 3, shows the horizontal and vertical velocity components (u, v) at depths of 10 mm and 16 mm, respectively. The former depth lies along the top of the rolls, where the flow is predominantly horizontal, while the latter depth traverses the centres of the rolls, where the flow is vertical. The data illustrate the cyclic variation in velocity with distance associated with successive Bénard rolls which alternate between clockwise and anticlockwise flow directions. As expected there is a horizontal shift between these curves of approximately a quarter of a wavelength. Apart from the difference in wavelength noted above, the form of the maximum vertical velocity distribution in the rolls is similar to that predicted theoretically, i.e. sinusoidal as shown in the figure. The agreement is reasonable, but there is evidence of some distortion in the data. Bergé (1975) has noted that at high supercritical Rayleigh numbers, where nonlinear effects due to fluid inertia are significant, harmonic distortion of the linear theory is to be expected. In particular,

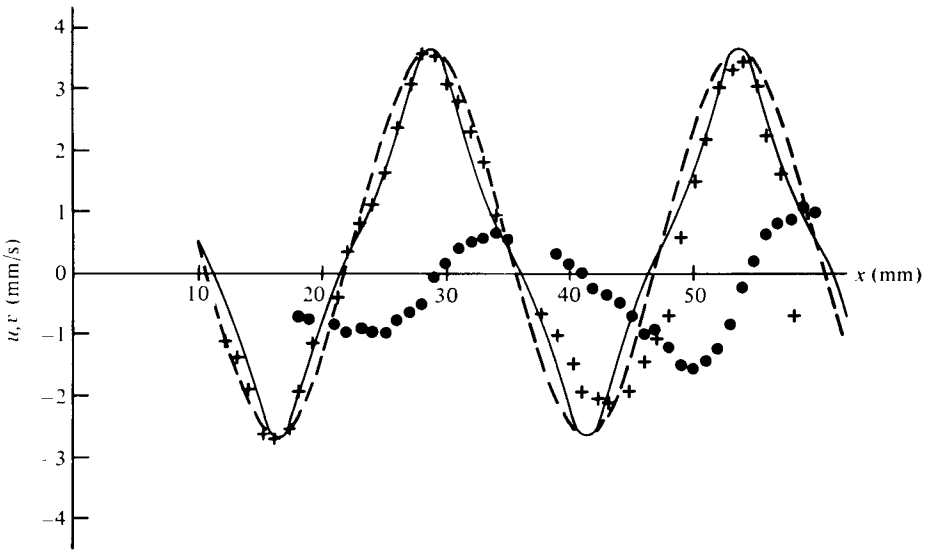

FIGURE 4. Horizontal velocity components at a depth of 10 mm (circles) and vertical velocity components at a depth of 16 mm (crosses) throughout the convection rolls. The broken line represents the sinusoidal form of the vertical velocity distribution while the solid line represents the sinusoidal form with an added third-harmonic component. $Ra = O(10^5)$.

the next significant term in the normal-mode analysis of the vertical velocity distribution is the third harmonic in phase with the fundamental mode. Such a harmonic distortion is also shown in figure 4. The amplitude of the harmonic components is taken as approximately 17 % of the fundamental on the basis of Bergé's results. The amplitude of the resulting periodic function has then been scaled to match that of the experimental observations. The agreement is seen to be a significant improvement over that with only the fundamental mode.

4. Conclusions

The LSP technique has been demonstrated to be capable of full-field velocity measurements of transient Bénard convection. It would be extremely difficult to make such measurements by any other technique. The measurements indicate that a two-dimensional roll pattern is established with the roll axes parallel to the short side of the cell and a roll wavelength about half that reported for steady-state Bénard convection. If the effective depth of the cell is reduced to account for the highly viscous layer near the top surface, the roll wavelength is approximately 25 % less than linear theory suggests. The measured velocities ranged up to 4 mm/s for an effective Rayleigh number $O(10^5)$ in aqueous glycerol. The maximum vertical velocity distribution is of sinusoidal form with a detectable third-harmonic component.

This new technique is well suited to a wide variety of applications because its range of sensitivity can easily be shifted by altering the pulse separation. Very little seeding of the liquid is required to produce side scattering sufficient for study of any interior plane within a substantial volume.

We wish to thank G. Ahlers for a number of informative discussions.

REFERENCES

BARKER, D. B. & FOURNEY, M. E. 1977 *J. Appl. Optics Lett.* **1**, 135.
BERGÉ, P. 1975 In *Fluctuations, Instabilities and Phase Transitions* (ed. T. Riste), p. 323. Plenum.
DAINTY, J. C. 1975 *Laser Speckle and Related Phenomena*. Springer.
DAVIS, S. H. 1967 *J. Fluid Mech.* **30**, 465.
DUBOIS, M. & BERGÉ, P. 1978 *J. Fluid Mech.* **85**, 641.
DUDDERAR, T. D. & SIMPKINS, P. G. 1977 *Nature* **270**, 45.
ELDER, J. W. 1965 *J. Fluid Mech.* **23**, 77.
FOSTER, T. D. 1965 *Phys. Fluids* **8**, 1770.
GROUSSON, R. & MALLICK, S. 1977 *Appl. Optics* **16**, 2334.
KOSCHMIEDER, E. L. 1966 *Beitr. Phys. Atmos.* **39**, 1.
KOSCHMIEDER, E. L. 1969 *J. Fluid Mech.* **35**, 527.
KOSCHMIEDER, E. L. 1974 *Adv. in Chem. Phys.* **26**, 177.
KRISHNAMURTI, R. 1968 *J. Fluid Mech.* **33**, 457.
PALM, E. 1975 *Ann. Rev. Fluid Mech.* **7**, 39.
PERRY, J. H. & CHILTON, C. H. 1973 *Chemical Engineers Handbook*, chap. 3. McGraw-Hill.
STORK, K. & MÜLLER, U. 1972 *J. Fluid Mech.* **54**, 599.

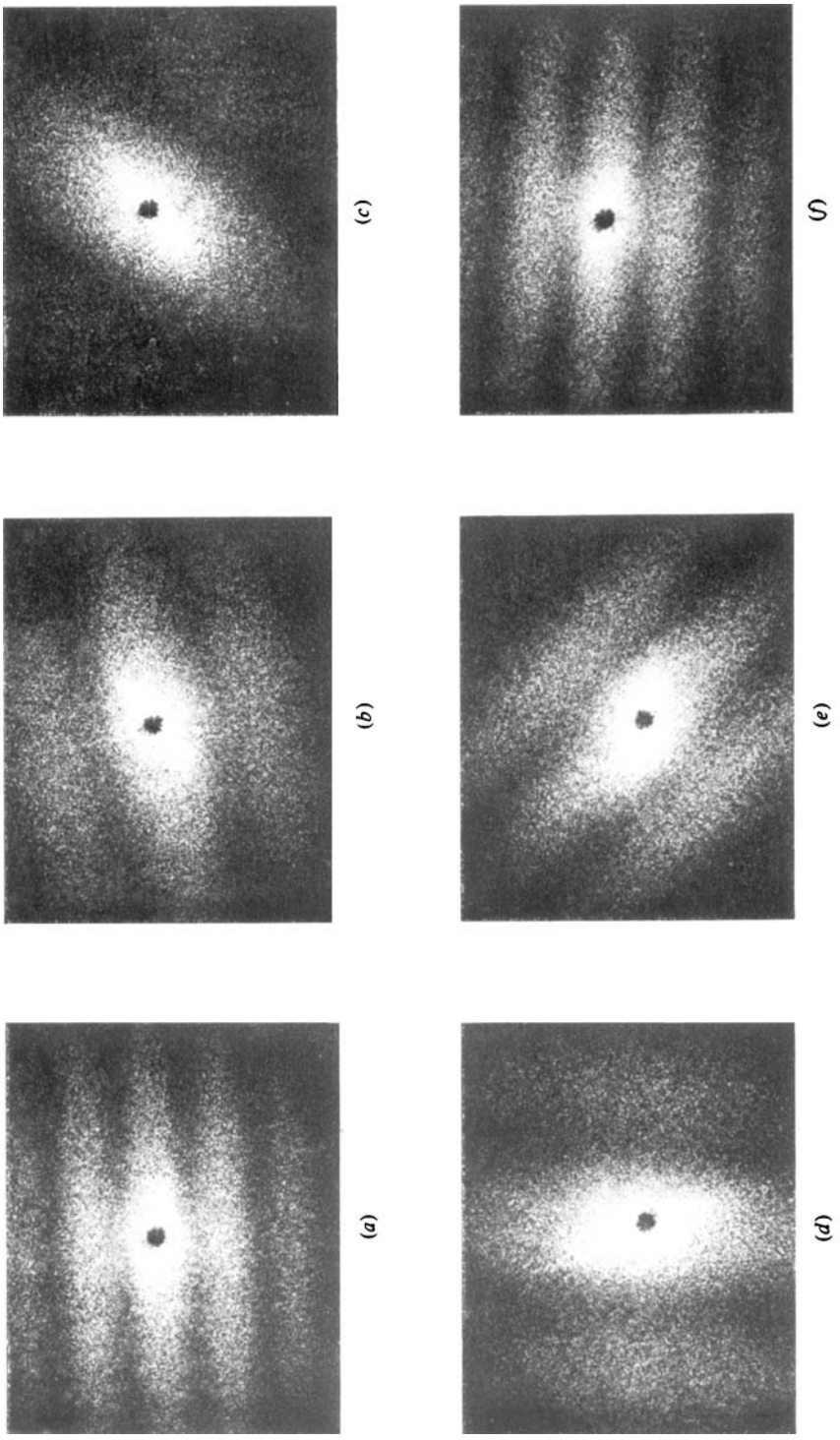

FIGURE 2. Typical diffraction fringe patterns from various horizontal locations along the cell at 20 mm depth. (*a*) $x = 43$ mm, $u = 1{\cdot}92$ mm/s; (*b*) $x = 44$ mm, $u = 1{\cdot}10$ mm/s; (*c*) $x = 46$ mm, $u = 0{\cdot}73$ mm/s; (*d*) $x = 47$ mm, $u = 0{\cdot}82$ mm/s; (*e*) $x = 49$ mm, $u = 1{\cdot}13$ mm/s; (*f*) $x = 52$ mm, $u = 1{\cdot}76$ mm/s. The black spot at the centre of each pattern is the shadow of the stop used to cut off the undiffracted portion of the interrogation beam.